

The PanK2 Genes of Mouse and Human Specify Proteins with Distinct Subcellular Locations

Roberta Leonardi¹, Yong-Mei Zhang¹, Athanasios Lydiki², Robert D. Stevens³, Olga R. Ilkayeva³, Brett R. Wenner³, James R. Bain³, Christopher B. Newgard³, Charles O. Rock¹, and Suzanne Jackowski¹

Department of Infectious Diseases, St Jude Children's Research Hospital, Memphis, Tennessee 38105¹, and Genome Biology Program DOE-Joint Genome Institute, Walnut Creek, California 94598², Sarah W. Stedman Nutrition and Metabolism Center, Duke University School of Medicine, Durham, North Carolina 27704³

¶Address correspondence to: Suzanne Jackowski, Ph.D., Department of Infectious Diseases, St Jude Children's Research Hospital, 332 N. Lauderdale, Memphis, Tennessee 38105-2794, Voice: 901 495-3494; Fax: 901 495-3099; Email: suzanne.jackowski@stjude.org

Abbreviations used are: CoA, coenzyme A; PanK, pantothenate kinase. Specific isoforms are numbered and preceded by 'm' for murine and 'h' for human; DTT, dithiothreitol; PBS, phosphate buffered saline; PKAN, PanK-associated neurodegeneration; PMSF, phenylmethylsulphonyl fluoride; qRT-PCR, real-time reverse transcriptase-polymerase chain reaction.

Running title: Regulation and localization of murine PanK2

Word count (Material and Methods) =

(Introduction, Results and Discussion) =

Keywords: pantothenate kinase, coenzyme A, mitochondria, neurodegeneration, acylcarnitine, and acetyl-CoA.

29
30
31
32
33
34
35
36
37
38
39
40
41
42
43
44
45

ABSTRACT

Coenzyme A (CoA) biosynthesis is initiated by pantothenate kinase (PanK) and tissue CoA levels are controlled through differential expression and allosteric regulation of the PanK isoforms. Mutations in human PanK2 (hPanK2) cause a neurodegenerative disorder termed PKAN; however, PKAN neuropathology is not recapitulated in *Pank2*^{-/-} mice. The distribution of the PanK isoforms differed between human and mouse tissues with the relative expression of PanK2 being higher in human brain compared to mouse brain. Comparative genomics analysis revealed that the acquisition of a mitochondrial targeting signal was limited to the PanK2 sequences from primates, and mouse PanK2 was localized in the cytosol. Both human and mouse PanK2 possessed similar biochemical properties, responding to inhibition by acetyl-CoA and activation by palmitoylcarnitines. Mouse brain had an abundance of the PanK2 allosteric activators, long-chain acylcarnitines, compared to liver, suggesting that the PanK2 isoform is more catalytically active in brain compared to liver. CoA levels were the same in tissues from wild-type and *Pank2*^{-/-} mice, and were highest in liver compared to brain and testes. The differences in the tissue-specific expression and cellular localization of the mouse PanK2 compared to human PanK2 may account for the inability to recapitulate the neuropathology of PKAN disease in the mouse model.

INTRODUCTION

46

47 CoA is an essential cofactor that plays a central metabolic role as the predominant acyl
48 group carrier in living organisms (23). The intracellular CoA levels vary depending on the
49 metabolic state of the cell and are tightly controlled to allow coordination of major anabolic and
50 catabolic pathways such as the tricarboxylic acid cycle and fatty acid metabolism (23,35).
51 Regulation of the cofactor concentration is achieved through feedback inhibition of pantothenate
52 kinase (PanK), the first enzyme in the biosynthetic pathway (28,29,34). PanK catalyzes the ATP-
53 dependent phosphorylation of pantothenate (vitamin B₅) to 4'-phosphopantothenate, and mammals
54 express four catalytically active isoforms that have different sensitivities to inhibition by free CoA or
55 CoA thioesters (30,40,41). A fifth potential isoform, PanK4, lacks the essential catalytic glutamate
56 residue present in all other enzymes (9) and is not a functional pantothenate kinase (39). PanKs
57 share a >80% identical catalytic core (10,30,40) attached to unrelated N-terminal extensions that
58 range from a few residues in the case of PanK1 β and PanK3 to ~100-200 residues in the case of
59 PanK1 α and PanK2. The N terminus of human PanK2 (hPanK2) directs it to the mitochondria.
60 hPanK2 is sequentially processed twice to yield a stable 48 kDa mature protein (10,17,19). The
61 sequences adjacent to the cleavage sites at residues 31 and 140, implicate the mitochondrial
62 processing peptidase in both cleavage steps. A hPanK2 construct starting at Leu111 (42) lacks
63 the first mitochondrial targeting signal, but is still processed and targeted to the mitochondria (17).
64 Removal of both signals causes the enzyme to mislocalize to the cytosol (10,17). A catalytically
65 active hPanK2 inside the mitochondria was irreconcilable with the high organelle CoA
66 concentration (13,37) until the discovery of palmitoylcarnitine as a positive regulator of hPanK2
67 (22). Palmitoylcarnitine releases the acetyl-CoA inhibition by competing for its binding site, and
68 this regulatory mechanism activates hPanK2 when the mitochondrial demand for CoA is high for β -
69 oxidation.

70 Pantothenate kinase-associated neurodegeneration (PKAN) is a rare autosomal recessive
71 disease caused by mutations in the *PANK2* gene (7,42). PKAN patients exhibit pathological
72 accumulation of iron in the brain, movement and speech defects and, in some cases, pigmentary

73 retinopathy (7,8,42). The classic form of the disease appears in childhood and is characterized by
74 a relentless progression of dystonia, dysarthria and rigidity. The classical disease is more
75 frequently associated with mutations that abolish or severely impair hPank2 activity. The atypical
76 form of PKAN has a later age at onset and a slower progression of speech-related and psychiatric
77 symptoms. Some hPank2 mutations result in protein misfolding or in truncated proteins; however,
78 others give rise to proteins with wild-type or significant residual catalytic activity (19,41). Active
79 hPank2 mutants exhibit the same regulatory properties and localization as the wild-type enzyme
80 (19,22,41), raising the question of what hPank2 function is compromised by these mutations. To
81 further complicate the picture, the connection between CoA biosynthesis/metabolism,
82 neurodegeneration and brain iron accumulation remains unclear. Reduced phosphorylation of
83 pantothenate may cause accumulation of cysteine, a CoA precursor, in regions of the brain that
84 are normally rich in non-heme iron. Cysteine oxidation in the presence of iron would then result in
85 free radical production and cell damage (17,42). Alternatively, oxidative stress caused by reduced
86 CoA-dependent energy production may selectively impact those tissues like the retina and the
87 brain characterized by a high metabolic demand and sensitivity to oxidative damage (7). There is
88 a growing body of evidence supporting the role of mitochondria in the pathogenesis of several
89 neurodegenerative diseases. Alzheimer's, Parkinson's and Huntington's share common
90 neurological features with PKAN (3,21,32,33) and mitochondrial defects lead to retinal
91 degeneration (4,31,38) and male sterility (24,25).

92 A significant conundrum in the field is that the *Pank2* knockout mice do not recapitulate the
93 neurological abnormalities that characterize the human phenotype, although they do exhibit retinal
94 degeneration and male sterility (20). We addressed this issue by comparing the tissue distribution,
95 gene structure, biochemical properties and subcellular localization of mPank2 and hPank2.
96 Although the biochemical regulatory properties of the two enzymes are indistinguishable,
97 differences in gene structure, subcellular localization of the proteins and relative abundance of
98 Pank2 in human and murine tissues suggest rationales for the similarities and differences in the
99 PKAN patients and *Pank2* knockout mice.

MATERIALS AND METHODS

100

101 **Materials.** Materials were purchased from the following suppliers: oligonucleotides and
102 probes from the Hartwell Center at the St. Jude Children's Research Hospital; Poly(A)⁺ RNAs from
103 mouse and human brain sections, human liver, brain and testes from Clontech; molecular biology
104 reagents from Qiagen; restriction enzymes and T4 DNA ligase from Promega; SuperScript™ II
105 RNase H⁻ reverse transcriptase, TRIZOL reagent, pCR2.1 and pcDNA3.1 vectors from Invitrogen;
106 Real-time PCR mix from Applied Biosystems; Bradford dye-binding protein assay solution from
107 Bio-Rad; D-[1-¹⁴C]pantothenate (specific activity, 55 mCi/mmol) from American Radiolabeled
108 Chemicals and [1-¹⁴C]lauric acid (specific activity 55 mCi/mmol) from GE Healthcare. All other
109 reagents were of analytical grade or better and were obtained from Sigma Chemical Co.

110 **Generation of *Pank2* knockout mice.** The targeting construct pPJ259 was generated by
111 cloning 3 fragments of mouse *Pank2* genomic DNA into vector pNEOtkLoxP. pPJ259 contained a
112 loxP site between a 3.5-kb genomic DNA and the TK and NEO selection cassettes, followed by a
113 second loxP site upstream of a 2.8-kb genomic DNA fragment containing exon 3, and by a third
114 one upstream of a 1.8-kb genomic DNA containing exon 4 (Fig. 1A). DraIII was used to linearize
115 the targeting vector prior to transfection into the embryonic stem cell lines derived from 129/SVEV
116 (Specialty Media), grown on mitotically inactivated mouse embryonic fibroblasts which carry
117 resistance to neomycin. Clones resistant to G418 were selected and screened by Southern blot
118 analysis using a 772-bp probe corresponding to a genomic DNA region outside the targeted
119 portion. Genomic DNA (10 μg) from individual ES cell clones was digested with BamHI and
120 Southern blot analysis was carried out as previously described (15). The presence of the third
121 loxP site was confirmed by PCR analysis. ES cells containing the recombined *Pank2* DNA at the
122 correct locus were injected into C57BL/6J blastocysts, which were then implanted into
123 pseudopregnant female mice by the St. Jude Transgenic Core Facility. Male offspring with 75 to
124 90% agouti color, the coat color contributed by the ES cells, were bred with C57BL/6J females.
125 Pups that were 100% agouti, indicating germ line transmission, were screened. Tail clips were
126 lysed and multiplex PCR analysis was used to genotype the mice using RED Extract-N-Amp PCR

127 kit (Sigma) and three primers: F (TTCCCTGCTTAGGTAGGATTGC), R1
128 (CCTTTGGACACCATGTAAATGAAC) and T (CCAAGTTCGGGTGAAGGC). The wild type allele
129 yielded a product of 618 bp, and the allele with the recombined *Pank2* yielded a product of 452 bp.
130 FVB/N-Tg(ACTB-cre)2Mrt/J mice expressing Cre recombinase under the human β -actin gene
131 promoter were utilized to generate complete deletion of *Pank2* by recombination of the first and
132 third loxP sites, resulting in the deletion of exon 3. A multiplex PCR analysis was used to genotype
133 the offsprings from the breeding of ACTB-cre mice with mice heterozygous for the recombined
134 *Pank2* using primers F, R1 and R2 (CCTCAACTCCTAGATCCAAACTG). A 618 bp product
135 indicated the presence of a wild type allele, and a 526 bp product indicated the presence of a
136 knockout allele. Heterozygous mice for *Pank2* knockout were bred to generate homozygous
137 knockout mice.

138 **Real time qRT-PCR analysis.** Total RNA was either purchased (mouse and human brain
139 sections, human liver, brain and testes) or isolated from whole brain and caudate nucleus region,
140 whole liver and testes of 2-3 wild type and *Pank2*^{-/-} mice, using the TRIZOL reagent according to
141 the manufacturer's instructions. Pelleted RNA was resuspended in nuclease-free water, digested
142 with DNase I to remove any contaminating genomic DNA, aliquoted, re-precipitated in ethanol and
143 stored at -20°C.

144 Synthesis of first-strand cDNA was obtained by reverse transcription using SuperScript™ II
145 RNase H⁻ reverse transcriptase, the RNA templates and random primers. Quantitative real-time
146 PCR of the human and murine PanK isoforms in each sample was performed in triplicate using the
147 ABI Prism® 7700 Sequence Detection System using primers and probes listed in Table 1. The
148 Taqman Human GAPDH and Rodent GAPDH Control Reagents (Applied Biosystems) were the
149 source of the primers and probes for quantitating the control GAPDH mRNA. All of the real-time
150 values were compared using the C_T method, and the amount of cDNA ($2^{-\Delta CT}$) was reported relative
151 to GAPDH.

152 **Cloning of the murine *Pank2*, dell transfection and preparation of cell lysates.** A 1.6
153 kb fragment encoding the long form of mPanK2 (10) was assembled from 3 ESTs (NCBI accession

154 numbers BG091057, CB247865 and BQ715345) and ligated into pcDNA3.1+ between EcoRI and
155 XbaI restriction sites. The resulting vector was named pPJ256.

156 HEK 293 and 293T cells were cultured in Dulbecco's modified Eagle's medium containing
157 10% fetal bovine serum (Atlanta Biologicals) and transfected with FuGENE 6 (Roche Applied
158 Science), as per manufacturer's instructions. For biochemical assays, 293T cells were transiently
159 transfected for 48 h with pPJ256 and pKM56, a pcDNA3.1-derived vector encoding the mature
160 hPanK2 (residues 141-570) (41). For immunofluorescence analysis, 293 cells were stably
161 transfected with pPJ256 and pKM4, a pcDNA3.1-derived vector encoding the mitochondrial
162 precursor hPanK2 (residues 1-570) (41), by selection in growth medium containing 600 µg/ml of
163 G418. Individual colonies were then expanded and screened for expression by western blotting
164 (see below). Transfected cells were collected, washed with PBS, and resuspended in lysis buffer
165 (10 mM Tris-HCl, pH 7.5, 1 mM EDTA, 10 mM NaF, and 5 µg/ml of leupeptin). After incubation on
166 ice for 1 h, cells were lysed by sonication. The lysate was centrifuged at 5,000 × g for 5 min at 4°C
167 to remove the unbroken cells. The supernatant was then either loaded on SDS-PAGE gels for
168 western blotting analysis or mixed with an equal volume of saturated ammonium sulfate for
169 subsequent activity assays. After incubation on ice for 1 h, the protein precipitate was collected by
170 centrifugation at 3,000 × g for 30 min. The precipitated protein was resuspended in the lysis buffer
171 without leupeptin and dialyzed against the same lysis buffer overnight at 4°C. The dialyzed protein
172 sample was stored in 50% glycerol at -20°C.

173 **Western blot detection and immunofluorescence.** Peptides corresponding to protein
174 stretches unique to mPanK2 (GESADSEARRRDPLRRR) and hPanK2 (EGRRQEPLRRRASSASV)
175 were synthesized and coupled to keyhole limpet hemocyanin by the Hartwell Center for
176 Biotechnology, St. Jude Children's Research Hospital, and sent to Rockland Inc. (Gilbertsville, PA)
177 to raise rabbit polyclonal antisera. Affinity purification of the polyclonal antibody was performed as
178 previously described (14,30). Heavy mitochondrial and cytosolic brain fractions (200 µg) were
179 loaded on 8% SDS-PAGE gels and the resolved proteins were electroblotted onto a polyvinylidene

180 difluoride membrane. The lysate from stably transfected cells (5 μ g) was mixed with the same
181 amount of cytosolic brain fraction from *Pank2* knockout mice and used as mPankK2 controls.
182 mPankK2 was detected by the mPankK2 antibody at a concentration of 0.1 μ g/ml. Horseradish
183 peroxidase-conjugated protein A was used as the secondary antibody at a dilution of 1:5,000. The
184 membranes were then stripped using a western blot recycling kit (Alpha Diagnostic International)
185 and reprobed with antibodies against the mitochondrial marker pyruvate dehydrogenase (PDH, E2
186 subunit, Molecular Probes) and the cytosolic marker β -actin (Sigma) used at concentrations of 2.5
187 μ g/ml and 5 μ g/ml, respectively, using horseradish peroxidase-conjugated anti-mouse IgG (GE
188 Healthcare) as secondary antibody at a dilution of 1:5,000. The immuno complexes were detected
189 using the ECL kit (GE Healthcare).

190 The localization of mPankK2 and the mitochondrial precursor hPankK2 was determined by
191 confocal microscopy, performed by the Scientific Imaging Shared Resource at St. Jude Children's
192 Research Hospital using a Zeiss LSM 510 META multiphoton microscope equipped with a Plan-
193 Neofluor 100x/1.3 oil immersion objective and controlled by Laser Scanning Microscope LSM 510
194 software (Ver.3.2, Carl Zeiss GmbH, Germany). Sample slides were prepared as described below
195 and washed with PBS between each incubation step. HEK 293 cells stably transfected with
196 pPJ256 and pKM4 were seeded in chamber slides (Lab-Tech II, Nalge Nunc International) and
197 allowed to adhere and grow for 16-24 h before being incubated with 250 nM MitoTracker red
198 CMXRos (Molecular Probes) for 30 min at 37°C. Cells were then fixed with 3.7% formaldehyde for
199 15 min at 37°C and permeabilized with 0.2% Triton X-100 for 5 min, before being incubated with
200 the mPankK2 and hPankK2 antibodies at concentrations of 0.03 and 0.005 μ g/ml, respectively, for 1
201 h at room temperature. Anti-rabbit IgG conjugated to Alexa Fluor 488 (Molecular Probes) diluted
202 1:250 was then added to the cells, followed by 1 h incubation at room temperature. The slides
203 were finally washed with PBS and mounted with ProLong Gold antifade reagent with DAPI
204 (Molecular Probes).

205 **Liver and brain fractionation.** Heavy mitochondria were isolated from wild type and
206 *Pank2* knockout mice liver or brain as described by Graham (6). All centrifugation steps and
207 fraction manipulation were conducted at 4°C. Briefly, freshly harvested organs from 4 wild type or
208 knock-out mice (~4 g) were homogenized in 12 ml of ice-cold LHM buffer (10 mM Hepes-KOH, pH
209 7.4, 0.2 M mannitol, 50 mM sucrose, 10 mM KCl and 1 mM EDTA) using a tissue grinder with a
210 motorized Teflon pestle (Glas-Col). The homogenate was centrifuged at 1,000 × *g* for 10 min to
211 remove nuclei, unbroken tissue and other cell debris. The supernatant was further centrifuged at
212 3,000 × *g* for 10 min and the pellet, consisting of heavy mitochondria, was washed twice with 10 ml
213 of LHM buffer, gently resuspended in 0.5 ml of the same buffer using a Dounce homogenizer and
214 finally aliquoted and stored at –80°C. The 3,000 × *g* supernatant was then sequentially centrifuged
215 at 12,000 × *g* for 15 min and 105,000 × *g* for 60 min to remove the light mitochondrial pellet and
216 microsomes, respectively. The resulting supernatant represented the cytosolic fraction.

217 **CoA measurements.** Extraction of CoA species from mouse whole tissues or liver
218 fractions and CoA assay were performed as described by Knights and Drew (18) with some
219 modifications. For whole liver, brain and testes, ~100 mg of tissue were homogenized in 0.4 ml of
220 chilled 6% HClO₄ containing 28 mM DTT. For liver fractions, 12 mg of mitochondrial or cytosolic
221 protein were mixed with an equal volume of 12% HClO₄ containing 56 mM DTT. The precipitated
222 proteins were removed by centrifugation and the pellet put aside for quantitation of long-chain CoA
223 thioesters. The supernatant was divided into two aliquots; one aliquot was adjusted to pH 7.5-8.5
224 with 2 M KOH and centrifuged to remove the insoluble potassium perchlorate formed, then used to
225 measure the amount of free CoA. The second aliquot was adjusted to pH 11-12 with 1 M KOH,
226 incubated for 1 h at room temperature to hydrolyze the short-chain CoA thioesters, then
227 neutralized with 0.6 M HCl and centrifuged. The supernatant was extracted 3 times with an equal
228 volume of hexane and the aqueous phase saved to determine the sum of free and short-chain
229 CoAs. The pellet containing the long-chain CoA thioesters from the first centrifugation step was
230 first washed with 0.6% perchloric acid containing 5 mM DTT, then with 5 mM DTT and finally

231 resuspended in the same solution. The CoA thioesters were hydrolyzed to free CoA and extracted
232 as described above. The reaction mixture for the CoA assay contained 200 mM Tris-HCl (pH 7.5),
233 8 mM MgCl₂, 0.1% Triton X-100, 2 mM EDTA, 20 mM NaF, 2.5 mM ATP, 10 μM [1-¹⁴C]lauric acid,
234 100 ng of *E. coli* acyl-CoA synthetase (0.0863 U) and extracts containing 25-400 pmol of free CoA,
235 in a total volume of 100 μl. The reaction was initiated by the addition of the enzyme, and the
236 reaction mixture was incubated at 35°C for 30 min, followed by the addition of 325 μl of
237 methanol:chloroform:n-heptane (1.41/1.25/1, v/v/v) and 25 μl of 0.4 M acetic acid. After the
238 mixture was mixed vigorously and centrifuged, [1-¹⁴C]lauryl-CoA in upper aqueous phase was
239 quantitated by counting in 3 ml of ScintiSafe 30% using Beckman LS 6500. The amount of free
240 CoA, short-chain and long chain acyl-CoA were combined and expressed as nmoles of total CoA/g
241 of wet tissue or nmoles of total CoA/g of protein in the case of liver mitochondrial and cytosolic
242 fractions.

243 **Acylcarnitine measurements.** Specimens of powdered liver and brain from wild type and
244 *Pank2*^{-/-} mice were homogenized in deionized water, and tissue extracts were prepared as
245 previously described (2,16). Measurement of acylcarnitines was done by direct-injection
246 electrospray tandem mass spectrometry, using a Quattro Micro LC-MS system (Waters-
247 Micromass) equipped with a model HTS-PAL autosampler (Leap Technologies), a model 1100
248 HPLC solvent delivery system (Agilent Technologies) and a data system running MassLynx
249 software.

250 **Pantothenate kinase activity assay.** The lysates of transfected HEK 293T cells were
251 obtained and treated as described above prior to measuring the pantothenate kinase activity (41).
252 In particular, the reaction mixtures contained 45 μM D-[1-¹⁴C]pantothenate (specific activity 27.5
253 mCi/mmol), 250 μM ATP pH 7.0, 10 mM MgCl₂, 0.1 M Tris-HCl pH 7.5 and 5 μg of protein. The
254 inhibitory effect of acetyl-CoA on the activity of mPank2 and mature hPank2 was determined by
255 including increasing concentrations of the compound in the reaction mixtures, as indicated. To
256 investigate the effect of palmitoylcarnitine on the acetyl-CoA inhibition, mPank2- and hPank2-

257 containing lysates were incubated with 62.5 and 93.8 nM of inhibitor, respectively, and increasing
258 concentrations of palmitoylcarnitine, as indicated. The residual pantothenate kinase activity in
259 *PanK2* knockout mice liver and brain cytosolic fractions was measured in reaction mixtures
260 containing 45 μ M D-[1-¹⁴C]pantothenate, 2.5 mM ATP pH 7.0, 10 mM MgCl₂, 0.1 M Tris-HCl pH
261 7.5, increasing amounts of protein, as indicated, and incubated for 15 min at 37°C. The activity of
262 the correspondent wild type fractions was determined in parallel under the same conditions.

263 **Bioinformatic analysis.** Genomic sequences for human (chromosome 20, NT_011387.8),
264 chimpanzee (chromosome 20, NW_001230484), cow (chromosome 13, NW_001493148.1), dog
265 (chromosome 24 NW_876277.1), cat (no chromosome information, AANGO1231943.1) and
266 mouse *PanK2* (chromosome 2, NW_000178.1) were retrieved from NCBI. The macaque genomic
267 sequence was retrieved from the sequencing center's website
268 (<http://www.hgsc.bcm.tmc.edu/projects/rmacaque/>). Sequence comparisons were performed using
269 the VISTA tools for comparative genomics (<http://genome.lbl.gov/vista/index.shtml>) (5).

270

RESULTS

271

272 **Generation of *Pank2* knockout mice.** *Pank2* knockout mice were first generated by
273 insertion of a selection cassette and disruption of the *Pank2* coding sequence (20). We
274 independently derived *Pank2*-deficient mice by deletion of a 2.8 kb DNA fragment containing exon
275 3 (Fig. 1A). Cre recombinase-dependent recombination of the first and third loxP sites resulted
276 also in the removal of the selection cassette along with exon 3. Embryonic stem cells were
277 transfected and selected, and chimeric mice were generated and bred by standard procedures
278 described under “Materials and Methods.” Mice heterozygous for *Pank2* were identified by PCR
279 analysis of tail DNA and bred to produce homozygous knockout mice (Fig. 1B). A reproductive
280 defect in the male *Pank2*-deficient mice precluded establishment of a homozygous breeding
281 colony, and routine mating of heterozygotes and genotyping of the pups was necessary to
282 propagate the *Pank2*^{-/-} mice. The testis phenotype of the knockout mice generated by deletion of
283 the *Pank2* gene was the same as described previously (20). Measurement of the testes weight
284 and histological analysis revealed significantly smaller testes and the absence of elongated mature
285 spermatozoa in the seminiferous tubules of these *Pank2* knockout mice (data not shown). Our
286 *Pank2*^{-/-} mice did not show a significant difference in weight at 6-8 weeks of age compared to
287 littermate controls.

288 **Tissue distribution of murine and human PanK isoforms.** A considerable number of
289 PKAN-causing *PANK2* mutations completely abolish hPanK2 enzymatic activity as a result of
290 frameshifts and premature stops in the enzyme sequence (8,42). Similarly, deletion of the mouse
291 *Pank2* exon 3 resulted in loss of enzymatic activity (see below). In spite of this, only retinal
292 degeneration is common between some of the PKAN patients and *Pank2* knockout mice, while the
293 neurodegeneration is unique to humans and the knockout mice exhibit azoospermia (20). We
294 compared the mRNA expression levels of the murine and human PanK isoforms in brain, testes
295 and in liver by quantitative RT-PCR. Expression of PanK4 was not taken into account because it
296 does not exhibit PanK activity (39). *PANK1* transcripts (*PANK1* α + *PANK1* β) dominated human
297 liver, whereas *Pank1* transcripts (*Pank1* α + *Pank1* β) in mouse liver were equivalent to *Pank3*

298 transcripts (Fig. 2) and relatively lower than in human. *PANK2* transcripts, on the other hand, were
299 relatively higher than *PANK1* and equivalent to *PANK3* in human brain, whereas *Pank2* transcripts
300 were low in mouse brain and *Pank3* expression was highest. *Pank2* transcripts were extremely
301 high in mouse testis, but were considerably less abundant in human testis. The ratio between
302 mouse *Pank2* and *Pank3* mRNAs was estimated at approximately 1:2 in brain and 1:1 in testes,
303 with *Pank2* representing 34% and 46% of the expressed isoforms in the two tissues, respectively
304 (Fig. 2A). Human *PANK2* transcripts were high in brain, equivalent to *PANK3*, and represented
305 45% of the *PANK* transcripts. Only 21% of the PanKs expressed in human testes were the *PANK2*
306 isoform (Fig. 2B). A detailed analysis of specific areas of the brain revealed a high expression of
307 human *PANK2* transcripts in the cerebellum, which controls motor coordination and movement,
308 and, as previously reported, in the caudate nucleus (10) (Fig. 2D). The overall abundance of the
309 murine *Pank* transcripts was lower than what was measured in the corresponding human brain
310 fractions (Fig. 2C), but the level of *Pank2* was higher in the cerebellum and cerebral cortex
311 compared to whole brain. These data revealed a correlation between the predominance of PanK2
312 expression and the physiological impact of loss of expression in tissues from human and mouse.

313 **PanK isoform expression and tissue CoA levels in wild-type and *Pank2* knockout**
314 **mice.** Loss of *Pank2* expression did not result in increased expression of either *Pank1* or *Pank3* in
315 the brain, testes or liver of *Pank2*^{-/-} mice (data not shown). Measurements of the CoA content
316 revealed that brain and testes from adult wild type mice contained 19 and 26 nmoles of total CoA
317 per gram of wet tissue, respectively, while the liver content was 6-fold higher (Fig. 3A). In each
318 tissue, 80-90% of the CoA pool was unesterified or “free.” No significant difference in the total or
319 free CoA content was found between organs from wild type and age-matched *Pank2* knockout
320 mice, indicating that the remaining PanK isoforms were able to maintain the CoA levels, even in
321 mouse testes. The CoA levels in mitochondria or cytosol also were the same in mouse wild-type
322 and knockout tissues, as exemplified by liver (Fig. 3B). These data indicated that loss of PanK2
323 expression did not reduce the CoA content, and that the activities of the PanK1 and PanK3
324 enzymes supplied the cellular CoA requirements of most cell types.

325 **Biochemical properties of mPank2 and tissue acylcarnitine measurements.** The
326 mature hPank2 (residues 141-570, 47.4 kDa) is similar to the predicted size of mPank2 (48.6
327 kDa). The N-terminus of the full length mPank2 is 122 residues shorter than the full-length human
328 homolog, therefore we compared the regulatory properties of mPank2 and the mature hPank2
329 expressed in the lysates of transfected HEK 293T cells. We found that the two enzymes were
330 similarly inhibited by acetyl-CoA and de-inhibited by palmitoylcarnitine (Fig. 4). The acetyl-CoA
331 IC_{50} s were estimated at 125 nM for hPank2 and 62.5 nM for mPank2, with slight variations from
332 preparation to preparation, and the concentration of palmitoylcarnitine that maximally restored the
333 activity was approximately 8 μ M in both cases (Figs. 4A and 4B). Free carnitine and short-chain
334 acylcarnitines are not activators of hPank2 (22), and the latter species were the major components
335 of the acylcarnitine pool in mouse liver obtained from animals fed standard chow (Fig. 6B).
336 Conversely, the mouse brain contained significantly higher amounts of myristoyl, palmitoyl, stearyl
337 and oleoylcarnitine (Fig. 5A). Organs from wild-type or *Pank2* knockout mice had comparable
338 acylcarnitine distributions (Fig. 5). Taken together, these data indicated that hPank2 and mPank2
339 had the same biochemical properties in humans and mice and pointed out that the contribution of
340 Pank2 to the total PanK activity in a specific tissue would depend on the molar ratio of inhibitors
341 and activator(s).

342 **Bioinformatic analysis of mammalian PanKs and localization of mPank2 in stably**
343 **transfected cells and brain fractions.** The complete coding sequence and the intron-exon
344 organization of the human *PANK2* gene was elucidated by Hörtnagel and coworkers (10) who
345 found an ATG start codon upstream of the CTG codon originally proposed as the start of the
346 hPank2 coding sequence (42). The N-terminus of the full length hPank2 protein contains a
347 mitochondrial targeting sequence (residues 1-140), which is responsible for the subcellular
348 localization of the enzyme and is encoded by exon 1. We compared the corresponding nucleotide
349 sequences from six organisms (humans, macaques, cows, dogs, cats and mice) using the VISTA
350 tools for comparative genomics (Fig. 6). The analysis revealed that while the macaque sequence
351 encoded an intact mitochondrial targeting sequence, most of the aligned nucleotide regions from

352 mouse, cat, dog and cow were not translated due to the presence of in-frame stop codons or the
353 absence of earlier start codons. In spite of the sequence similarity, the predicted ATG start codon
354 in these organisms corresponded to residue 123 of hPanK2, thus excluding most of the
355 mitochondrial targeting sequence. The targeting sequence was also found in the predicted
356 chimpanzee PanK2 protein (NCBI accession number XP_001163366), which was not included in
357 the VISTA analysis because of the poor quality of the DNA data in the region aligned. These data
358 suggest that emergence of a mitochondrial targeting sequence occurred following the divergence
359 of primates.

360 The bioinformatics data prompted us to re-examine the subcellular localization of hPanK2
361 and mPanK2. Stable cell clones overexpressing the full-length forms of hPanK2 and mPanK2
362 were generated, and the localization of the two proteins was investigated *in situ* by confocal
363 immunofluorescence microscopy using mPanK2- and hPanK2-specific antibodies. Unlike the
364 mitochondrial hPanK2 (Fig. 7, E-H), mPanK2 was found in the cytosol (Fig. 7, A-B). These results
365 were the same in either the human cell line, HEK 293T (Fig. 7), or the mouse cell line, NIH 3T3
366 (data not shown). The subcellular location of mPanK2 was confirmed by western blotting analysis
367 of cytosolic and mitochondrial fractions obtained from wild-type and knockout mouse brains and
368 livers using the mPanK2-specific antibody, along with antibodies that recognize the β -actin marker
369 protein for cytosol and the pyruvate dehydrogenase marker for mitochondria (Fig. 8A). mPanK2
370 was found exclusively in wild type cytosol, not in mitochondria, and the size of the endogenous
371 protein matched the size of the full-length expressed mPanK2 predicted from genomic analysis
372 (48.6 kDa).

373 To corroborate these results, we measured the total PanK activity in the cytosol and heavy
374 mitochondrial fractions isolated from mouse brain and liver. PanK activity was detected in the
375 cytosolic (Fig. 8A), but not in the mitochondrial fractions. The PanK enzymatic assay cannot
376 discriminate between the various isoforms, but comparison of the cytosolic activity from wild-type
377 and knockout mice showed a 10- and 2-fold reduction in knockout brain and liver, respectively,
378 under the conditions described under Materials and Methods. The residual PanK activity in

379 knockout brain and liver was due to the expression of the PanK1 and PanK3 isoforms, and
380 knockout brain showed a greater decrease in activity, consistent with the higher relative
381 abundance of mPanK2 in wild-type brain (32%) compared to liver (9%) (Fig. 2A). The total PanK
382 enzymatic activity in wild-type brain was almost as high as in liver, despite somewhat lower PanK
383 expression levels (Fig. 2A), and showed a greater proportional decrease in the knockout brain,
384 indicating a greater PanK2 contribution in this tissue, possibly due to a higher concentration of
385 long-chain acylcarnitine activators (Fig. 5A).

386

387

DISCUSSION

388 A major finding of this study is that mouse PanK2 is a cytosolic protein in contrast to the
389 mitochondrial localization of the human enzyme. The PanK2 proteins from human and mouse are
390 homologous due to the strong similarity between their catalytic cores, and accordingly their
391 biochemical and regulatory properties are similar. Both proteins are equivalently sensitive to
392 feedback inhibition by acetyl-CoA, which is relieved by long-chain acylcarnitine (Fig. 4)(22). The
393 amino terminal sequences of the PanK2s from human and mouse are distinctly different; however,
394 and the mouse protein does not localize to the mitochondria (Figs. 7 and 8). In contrast to
395 hPanK2, the analysis of the mPanK2 sequence with PSORTII (11) does not indicate a
396 mitochondrial localization for the enzyme, but rather it is predicted to localize to the cytosol. The
397 cytosolic location of mPanK2 was directly observed using in situ microscopy of stably expressed
398 protein and was confirmed by subcellular fractionation of the endogenous PanK2 in mouse brain
399 and liver (Figs.7 and 8). mPanK2 is not processed and the molecular size of mPanK2 in vivo
400 corresponds to the size predicted by expression from the first in-frame Met codon (48.6 kDa),
401 rather than an upstream Leu codon (50.2 kDa) that was initially proposed as the start site (17).
402 These data are not in agreement with previous reports that concluded both mouse and human
403 PanK2 proteins as associated with mitochondria based on the immunolocalization of hPanK2 and
404 mPanK2 in transiently transfected COS7 cells and tissue sections. However, our examination of
405 the same data suggest a significant difference between the localization of the two proteins (17,20).

406 Analysis of the PanK2 protein sequences from available mammalian genomes shows that only
407 primates evolved the mitochondrial targeting mechanism, suggesting that this feature is related to
408 the more complex neurological development in primates.

409 These results provide a rationale for why the phenotype of the *Pank2* knockout mouse does
410 not include an overt neurological disease that is characteristic of PKAN patients, including those
411 with null mutations in the *PANK2* gene (20). The possibility of interference of the gene insertion
412 cassette on the transcriptional activity of flanking chromosomal regions was ruled out by the
413 independent isolation of a *Pank2*^{-/-} mouse using a gene deletion strategy that removed the
414 selection cassette as well as exon 3. The loss of mPanK2 activity in *Pank2*^{-/-} mice is not
415 accompanied by an increase in the expression level of the other isoforms, and does not lead to
416 decreased CoA levels in brain, liver or testes. These data indicate that the other PanK isoforms
417 are able to maintain the homeostatic cofactor concentration in most tissues of the knockout
418 animals. This outcome is not completely unexpected since all PanKs are regulated through
419 feedback inhibition by CoA thioesters and a drop in the inhibitor levels would stimulate the activity
420 of the remaining isoforms. However, the fact that the *Pank2* knockout mice exhibit a defect in
421 sperm maturation suggests cell-type specific isoform expression has a selective effect on
422 development of selected lineages. No data are available on the CoA content in normal and PKAN-
423 affected brains, although like the mouse testis, these data may not reveal deficiencies in
424 specialized cell types. There was a correlation between the relative abundance of PanK2
425 transcripts and the tissue-specific dysfunction related to the loss of its expression. Mouse PanK2
426 constituted a smaller proportion of the mRNA species in most brain regions compared to the
427 predominant expression of hPanK2 in human brain. In particular, the human caudate nucleus,
428 which is part of the basal ganglia where iron accumulation is noted in many PKAN patients (36),
429 has a high proportion of *PANK2* transcripts, whereas the mouse caudate nucleus has a relatively
430 lower amount (Fig. 2C). On the other hand, *Pank2* expression is high in mouse testes (Fig. 2A),
431 where loss of its expression impacted the development of spermatozoa in the knockout animals.

432 The intramitochondrial concentration of CoA species is estimated to be in the millimolar
433 range, thousands of fold higher than what would inhibit the PanK2 enzymes (13,37). Carnitine is
434 also an abundant metabolite (12) and this pool is made up of free carnitine, short- and long-chain
435 carnitine esters. Compositional analysis of the acylcarnitines present in mouse liver and brain
436 revealed a higher long-chain to short-chain ratio in the brain, suggesting that in non-stressed
437 conditions on a standard diet, the basal activity of mPanK2 is higher in brain due to the higher
438 concentration of activator. The ratio of free carnitine to acylcarnitine varies also as a function of
439 the availability of fatty acids destined for β -oxidation and energy production (26,27). The cytosolic
440 location of mPanK2 would not prevent its activation by acylcarnitine, but also would not optimize
441 the response. In the absence of PanK2 expression, a prompt response to the mitochondrial
442 demand for CoA may not be satisfied, potentially disrupting or delaying the function of the
443 organelle, particularly in human neural tissue where the PanK2 is highly expressed and localizes to
444 the site of palmitoylcarnitine synthesis. We recently proposed a model that places hPanK2 in the
445 intramembrane space (22), the submitochondrial compartment where palmitoyl-CoA is converted
446 to palmitoylcarnitine; the high local concentration of palmitoylcarnitine would efficiently activate
447 hPanK2 making the enzyme a more sensitive sensor of the mitochondrial demand for CoA.
448 However, because palmitoylcarnitine diffuses into the cytosol, the same sensory mechanism would
449 work even if the enzyme is localized in this compartment, as is the case with mPanK2 and all other
450 metazoan PanKs, with the exception of primates. Therefore, our working hypothesis is that the
451 biochemical function of mPanK2 and hPanK2 is the same and does not strictly require
452 mitochondrial localization.

453 Chemical knockout of the total PanK activity dramatically reduces CoA levels in liver and
454 significantly affects mitochondrial function and morphology (39). Reduction or elimination of
455 PanK2 activity in PKAN patients results in neurological symptoms that are common to several
456 other neurodegenerative disorders associated with mitochondrial dysfunction (21,32,33). This
457 correlation between potential mitochondrial dysfunction and hPanK2 activity has been attributed to
458 the unique localization of hPanK2 (10,19). However, defects in mitochondrial respiration or

459 alteration of the transmembrane potential can also be the underlying cause of the male sterility and
460 retinal degeneration (4,24,25,31,38) observed in the *Pank2* knockout mice (20) and the *fumble* fly
461 (1), both of which are deficient in a cytosolic enzyme. Thus, it appears that this correlation is not
462 linked to the specific localization of PanK2. Instead, knocking out of a PanK isoform would likely
463 cause a mitochondrial dysfunction-related phenotype in cell types where the expression of one
464 isoform predominates and the corresponding reduction in CoA level is less likely to be restored by
465 the activation of the remaining isoforms.

466

467

ACKNOWLEDGEMENTS

468 We thank Pamela Jackson, Karen Miller, Caroline Pate, Jina Wang and Ruobing Zhou, for
469 their expert technical assistance. This work was supported by National Institutes of Health Grants
470 GM 62896 (S.J.), DK58398 (C.B.N.), Cancer Center (CORE) Support Grant CA 21765, and the
471 American Lebanese Syrian Associated Charities.

472

REFERENCES

- 473
474
475 1. **Afshar, K., P. Gonczy, S. DiNardo, and S. A. Wasserman.** 2001. *fumble* encodes a pantothenate
476 kinase homolog required for proper mitosis and meiosis in *Drosophila melanogaster*. *Genetics*
477 **157**:1267-1276.
- 478 2. **An, J., D. M. Muoio, M. Shiota, Y. Fujimoto, G. W. Cline, G. I. Shulman, T. R. Koves, R. Stevens,**
479 **D. Millington, and C. B. Newgard.** 2004. Hepatic expression of malonyl-CoA decarboxylase
480 reverses muscle, liver and whole-animal insulin resistance. *Nat. Med.* **10**:268-274.
- 481 3. **Dobson, J.** 2004. Magnetic iron compounds in neurological disorders. *Ann. N. Y. Acad. Sci.* **1012**:183-
482 192.
- 483 4. **Finsterer, J.** 2006. Central nervous system manifestations of mitochondrial disorders. *Acta Neurol.*
484 *Scand.* **114**:217-238.
- 485 5. **Frazer, K. A., L. Pachter, A. Poliakov, E. M. Rubin, and I. Dubchak.** 2004. VISTA: computational
486 tools for comparative genomics. *Nucleic Acids Res.* **32**:W273-W279.
- 487 6. **Graham, J. M.** 1999. Isolation of Mitochondria from Tissues and Cells by Differential Centrifugation, p.
488 3.3.1-3.3.15. *In* J. S. Bonifacino, M. Dasso, J. B. Harford, J. Lippincott-Schwartz, and K. M. Yamada
489 (ed.), *Current Protocols in Cell Biology*. John Wiley & Sons, Inc..
- 490 7. **Hayflick, S. J.** 2003. Unraveling the Hallervorden-Spatz syndrome: pantothenate kinase-associated
491 neurodegeneration is the name. *Curr. Opin. Pediatr.* **15**:572-577.
- 492 8. **Hayflick, S. J., S. K. Westaway, B. Levinson, B. Zhou, M. A. Johnson, K. H. Ching, and J.**
493 **Gitschier.** 2003. Genetic, clinical, and radiographic delineation of Hallervorden-Spatz syndrome. *N.*
494 *Engl. J. Med.* **348**:33-40.
- 495 9. **Hong, B. S., M. K. Yun, Y.-M. Zhang, S. Chohnan, C. O. Rock, S. W. White, S. Jackowski, H. W.**
496 **Park, and R. Leonardi.** 2006. Prokaryotic type II and type III pantothenate kinases: The same
497 monomer fold creates dimers with distinct catalytic properties. *Structure* **14**:1251-1261.
- 498 10. **Hörtnagel, K., H. Prokisch, and T. Meitinger.** 2003. An isoform of hPANK2, deficient in pantothenate
499 kinase-associated neurodegeneration, localizes to mitochondria. *Hum. Mol. Genet.* **12**:321-327.
- 500 11. **Horton, P. and K. Nakai.** 1997. Better prediction of protein cellular localization sites with the k nearest
501 neighbors classifier. *Proc. Int. Conf. Intell. Syst. Mol. Biol.* **5**:147-152.
- 502 12. **Hutter, J. F., C. Alves, and S. Soboll.** 1990. Effects of hypoxia and fatty acids on the distribution of
503 metabolites in rat heart. *Biochim. Biophys. Acta* **1016**:244-252.
- 504 13. **Idell-Wenger, J., L. Grotyohann, and J. R. Neely.** 1978. Coenzyme A and carnitine distribution in
505 normal and ischemic hearts. *J. Biol. Chem.* **253**:4310-4318.
- 506 14. **Jackowski, S.** 1994. Coordination of membrane phospholipid synthesis with the cell cycle. *J. Biol.*
507 *Chem.* **269**:3858-3867.
- 508 15. **Jackowski, S., J. E. Rehg, Y.-M. Zhang, J. Wang, K. Miller, P. Jackson, and M. A. Karim.** 2004.
509 Disruption of CCT β 2 expression leads to gonadal dysfunction. *Mol. Cell. Biol.* **24**:4720-4733.
- 510 16. **Jensen, M. V., J. W. Joseph, O. Ilkayeva, S. Burgess, D. Lu, S. M. Ronnebaum, M. Odegaard, T.**
511 **C. Becker, A. D. Sherry, and C. B. Newgard.** 2006. Compensatory responses to pyruvate
512 carboxylase suppression in islet β -cells: preservation of glucose-stimulated insulin secretion. *J. Biol.*
513 *Chem.* **281**:22341-22351.
- 514 17. **Johnson, M. A., Y. M. Kuo, S. K. Westaway, S. M. Parker, K. H. Ching, J. Gitschier, and S. J.**
515 **Hayflick.** 2004. Mitochondrial localization of human PANK2 and hypotheses of secondary iron
516 accumulation in pantothenate kinase-associated neurodegeneration. *Ann. N. Y. Acad. Sci.* **1012**:282-
517 298.
- 518 18. **Knights, K. M. and R. Drew.** 1988. A radioisotopic assay of picomolar concentrations of coenzyme A
519 in liver tissue. *Anal. Biochem.* **168**:94-99.
- 520 19. **Kotzbauer, P. T., A. C. Truax, J. Q. Trojanowski, and V. M. Y. Lee.** 2005. Altered neuronal
521 mitochondrial coenzyme A synthesis in neurodegeneration with brain iron accumulation caused by
522 abnormal processing, stability, and catalytic activity of mutant pantothenate kinase 2. *J. Neurosci.*
523 **25**:689-698.
- 524 20. **Kuo, Y. M., J. L. Duncan, S. K. Westaway, H. Yang, G. Nune, E. Y. Xu, S. J. Hayflick, and J.**
525 **Gitschier.** 2005. Deficiency of pantothenate kinase 2 (*Pank2*) in mice leads to retinal degeneration
526 and azoospermia. *Hum. Mol. Genet.* **14**:49-57.
- 527 21. **Kwong, J. Q., M. F. Beal, and G. Manfredi.** 2006. The role of mitochondria in inherited
528 neurodegenerative diseases. *J. Neurochem.* **97**:1659-1675.
- 529 22. **Leonardi, R., C. O. Rock, S. Jackowski, and Y.-M. Zhang.** 2007. Activation of human mitochondrial
530 pantothenate kinase 2 by palmitoylcarnitine. *Proc. Natl. Acad. Sci. U. S. A.* **104**:1494-1499.

- 531 23. **Leonardi, R., Y.-M. Zhang, C. O. Rock, and S. Jackowski.** 2005. Coenzyme A: Back in action. *Prog.*
532 *Lipid Res.* **44**:125-153.
- 533 24. **Nakada, K., A. Sato, K. Yoshida, T. Morita, H. Tanaka, S. Inoue, H. Yonekawa, and J. Hayashi.**
534 2006. Mitochondria-related male infertility. *Proc. Natl. Acad. Sci. U. S. A.* **103**:15148-15153.
- 535 25. **Perl, A., Y. Qian, K. R. Chohan, C. R. Shirley, W. Amidon, S. Banerjee, F. A. Middleton, K. L.**
536 **Conkrite, M. Barcza, N. Gonchoroff, S. S. Suarez, and K. Banki.** 2006. Transaldolase is essential
537 for maintenance of the mitochondrial transmembrane potential and fertility of spermatozoa. *Proc.*
538 *Natl. Acad. Sci. U. S. A.* **103**:14813-14818.
- 539 26. **Ramsay, R. R. and A. Arduini.** 1993. The carnitine acyltransferases and their role in modulating acyl-
540 CoA pools. *Arch. Biochem. Biophys.* **302**:307-314.
- 541 27. **Ramsay, R. R. and V. A. Zammit.** 2004. Carnitine acyltransferases and their influence on CoA pools
542 in health and disease. *Mol. Aspects Med.* **25**:475-493.
- 543 28. **Robishaw, J. D., D. A. Berkich, and J. R. Neely.** 1982. Rate-limiting step and control of coenzyme A
544 synthesis in cardiac muscle. *J. Biol. Chem.* **257**:10967-10972.
- 545 29. **Robishaw, J. D. and J. R. Neely.** 1984. Pantothenate kinase and control of CoA synthesis in heart.
546 *Am. J. Physiol. Cell.* **246**:H532-H541.
- 547 30. **Rock, C. O., M. A. Karim, Y.-M. Zhang, and S. Jackowski.** 2002. The murine *Pank1* gene encodes
548 two differentially regulated pantothenate kinase isozymes. *Gene* **291**:35-43.
- 549 31. **Sano, Y., A. Furuta, R. Setsuie, H. Kikuchi, Y. L. Wang, M. Sakurai, J. Kwon, M. Noda, and K.**
550 **Wada.** 2006. Photoreceptor cell apoptosis in the retinal degeneration of Uchl3-deficient mice. *Am. J.*
551 *Pathol.* **169**:132-141.
- 552 32. **Schapira, A. H.** 2002. Primary and secondary defects of the mitochondrial respiratory chain. *J. Inherit.*
553 *Metab. Dis.* **25**:207-214.
- 554 33. **Schapira, A. H.** 2006. Mitochondrial disease. *Lancet* **368**:70-82.
- 555 34. **Song, W.-J. and S. Jackowski.** 1994. Kinetics and regulation of pantothenate kinase from
556 *Escherichia coli*. *J. Biol. Chem.* **269**:27051-27058.
- 557 35. **Tahiliani, A. G. and C. J. Beinlich.** 1991. Pantothenic acid in health and disease. *Vitam. Horm.*
558 **46**:165-228.
- 559 36. **Thomas, M., S. J. Hayflick, and J. Jankovic.** 2004. Clinical heterogeneity of neurodegeneration with
560 brain iron accumulation (Hallervorden-Spatz syndrome) and pantothenate kinase-associated
561 neurodegeneration. *Mov. Disord.* **19**:36-42.
- 562 37. **Williamson, J. and B. Corkey.** 1979. Assay of citric acid cycle intermediates and related compounds-
563 uptake with tissue metabolite levels and intracellular distribution. *Methods Enzymol.* **55**:200-222.
- 564 38. **Zhang, X., D. Jones, and F. Gonzalez-Lima.** 2002. Mouse model of optic neuropathy caused by
565 mitochondrial complex I dysfunction. *Neurosci. Lett.* **326**:97-100.
- 566 39. **Zhang, Y.-M., S. Chohnan, K. G. Virga, R. D. Stevens, O. R. Ilkayeva, B. R. Wenner, J. R. Bain, C.**
567 **B. Newgard, R. E. Lee, C. O. Rock, and S. Jackowski.** 2007. Chemical knockout of pantothenate
568 kinase reveals the metabolic and genetic program responsible for hepatic coenzyme A homeostasis.
569 *Chem. Biol.* **14**:291-302.
- 570 40. **Zhang, Y.-M., C. O. Rock, and S. Jackowski.** 2005. Feedback regulation of murine pantothenate
571 kinase 3 by coenzyme A and coenzyme A thioesters. *J. Biol. Chem.* **280**:32594-32601.
- 572 41. **Zhang, Y.-M., C. O. Rock, and S. Jackowski.** 2006. Biochemical properties of human pantothenate
573 kinase 2 isoforms and mutations linked to pantothenate kinase-associated neurodegeneration. *J.*
574 *Biol. Chem.* **281**:107-114.
- 575 42. **Zhou, B., S. K. Westaway, B. Levinson, M. A. Johnson, J. Gitschier, and S. J. Hayflick.** 2001. A
576 novel pantothenate kinase gene (*PANK2*) is defective in Hallervorden-Spatz syndrome. *Nat. Genet.*
577 **28**:345-349.
- 578

579

580

TABLE I

581

Primers and Probes for mouse and human Pank RT-PCR

582

| Gene | Forward Primer (5'-3') | Reverse Primer (5'-3') | Probe (5'-3') ¹ |
|--------------|---------------------------|----------------------------|--------------------------------------|
| <i>Pank1</i> | ATGACTTGCCCTCATTTGCAT | TGGGAGCCCCTCCAAATT | CCGTATGAAGGGCAGCAAACCC |
| <i>Pank2</i> | TTGGGCATACGTGGAGCTTT | TCTCACATACATTTCAACAGGACAAG | TGGACTIONCCACCAGCAGCTGAC |
| <i>Pank3</i> | CTAAGGAACGCCTGCCATTC | CTTTGGTTCCCAGTGACAGACA | AGCTGATCCAGAAACCGCAGTCA |
| <i>PANK1</i> | TGAGCTTATTGTTGAAAGGGATTTT | GGTGCTCAGAAGGCAGAGAAA | AGGACAGAACAATTACTCCATGAT GAATCTTC |
| <i>PANK2</i> | AGAGCTGCTCTGTGTTCAAGTTGA | CGCATAGTAGCCTGCCTTACATT | AGCAAGTTCAAACAGGACACAAAA CCA |
| <i>PANK3</i> | CACCATGCTCTTATCTCGCACTT | TTGAAGGCAGAGGGCTCAAC | TCCCCTTGCTGAATCTGG |

583 ¹All probes used 6-FAM (6-carboxyfluorescein) as reporter and BHQ1 (black hole quencher 1) as
584 quencher.

585

FIGURE LEGENDS

586 **FIG. 1.** Generation of *Pank2* knockout mice by homologous recombination and cre-
587 mediated deletion. (A) Organization of the *Pank2* locus and screening strategy for the targeting
588 construct. ES cells containing the recombinant *Pank2* at the correct locus were identified by
589 Southern blotting analysis using the BamHI restriction enzyme, B, and a 722 bp probe outside the
590 targeted portion. LoxP sites (▶) allowed for the cre-mediated deletion of the selection cassette
591 and exon 3. (B) Genotyping was accomplished by PCR using primers F, R and R2 as described
592 under “Materials and Methods.” A 618 and 526 bp products indicated the presence of a wild type
593 allele and knockout allele, respectively.

594

595 **FIG. 2.** PanK isozyme expression in murine and human tissues. (A and B) The abundance
596 of murine (A) or human (B) PanK isoform mRNAs was determined in brain, testes and liver by real
597 time RT-PCR. (C and D) The same analysis was conducted on mRNA from specific regions of the
598 murine (C) and human (D) brain. PanK2 is highly abundant in mouse testes and human brain. All
599 RNA samples were purchased with the exception of murine RNA from whole brain, testes and liver
600 and caudate nucleus that was extracted from 2-3 wild type mice as described under “Materials and
601 Methods.” Individual samples were analyzed in triplicate, averaged and plotted relative to mouse
602 or human glyceraldehyde-3-phosphate dehydrogenase mRNA. Data obtained from different mice
603 were then further averaged. All data are plotted as mean \pm the standard error.

604

605 **FIG. 3.** Measurement of total CoA in murine whole tissues and liver fractions. (A) Total
606 CoA levels were determined in brain, liver and testes obtained from wild type (black bars) and
607 *Pank2* knockout (white bars) mice as described under Materials and Methods.” (B) Mitochondrial
608 and cytosolic fractions were isolated from the livers of wild type (black bars) and *Pank2* knockout
609 (white bars) mice and the total CoA measured. No significant difference was observed CoA levels

610 of whole tissues or liver fractions from wild type and *Pank2*-deficient mice. The data represent the
611 average of three independent experiments \pm the standard error.

612

613 **FIG. 4.** Regulatory properties of mPanK2 and hPanK2. (A) Acetyl-CoA inhibited both
614 mPanK2 (●) and the mature form of hPanK2 (41) (○) with similar IC_{50} of 62.5 and 125 nM,
615 respectively. (B) Inhibition by acetyl-CoA was released by the addition of palmitoylcarnitine. The
616 enzymes were incubated with fixed concentrations of acetyl-CoA corresponding to the respective
617 IC_{50} s and with increasing amounts of the activator. The data represent the average of two
618 independent experiments \pm the standard error.

619

620 **FIG. 5.** Analysis of the acylcarnitine pool in mouse tissues. The composition of the
621 acylcarnitine pool present in the brain (A) and liver (B) of wild type and *Pank2* knockout mice was
622 determined by electrospray mass spectroscopy as described under "Materials and Methods." The
623 brain and liver acylcarnitine pools showed significantly different compositions, with long-chain
624 acylcarnitines, known activators of PanK2, were abundant in the brain but not in the liver. Loss of
625 mPanK2 did not cause a remodeling of the acylcarnitine pool.

626

627 **FIG. 6.** DNA level sequence similarity of the 5-untranslated regions and exon 1 of six
628 mammals. Genomic DNA sequences were aligned using the VISTA set of tools for comparative
629 genomics and using human *PANK2* as the reference sequence. Black arrows indicate the
630 positions of the predicted start codons in the corresponding organisms. The region corresponding
631 to the human mitochondrial targeting signal has been shadowed and the positions of the
632 mitochondrial processing peptidase cleavage sites (19) are indicated by the scissor symbol at the
633 top.

634

635 **FIG. 7.** Subcellular localization of mPanK2 and hPanK2. (A-C) Stably transfected HET 293
636 cells expressing mPanK2, (E-G) the mitochondrial precursor form of hPanK2 (41) or containing (D

637 and H) the empty vector were cultured and prepared for immunofluorescence as described under
638 'Materials and Methods'. (A and D) Cells were incubated with MitoTracker red CMXRos and with
639 specific antibodies against (B and F) mPank2 or (E and H) hPank2, followed by incubation with
640 anti-rabbit IgG conjugated to Alexa Fluor 488 green; nuclei were stained with DAPI (blue). Panels
641 C and D show the merged images for mPank2 and empty vector, respectively; panels G and H
642 show the merged images for hPank2 and empty vector, respectively. hPank2 localized to the
643 mitochondria, while mPank2 was found in the cytosol.

644

645 **FIG. 8.** Cytosolic localization of mPank2 confirmed by activity assays and western blotting
646 analysis. (A) Western blot using 200 μ g of brain mitochondrial and cytosolic fraction protein from
647 wild type and *Pank2* knockout mice and the specific mPank2 antibody. 195 μ g of cytosolic protein
648 from knockout mice were mixed with 5 μ g of lysate protein from stably transfected HET 293 cells
649 expressing mPank2 and used as a control. (B) The total PanK activity was measured in liver (■,
650 □) and brain (●, ○) cytosolic fractions obtained from wild type (■, ●) and *Pank2* knockout (□, ○)
651 mice as described under 'Materials and Methods'. Cytosolic fractions from knockout mice showed
652 a significantly lower activity than those from wild type, consistent with the absence of mPank2 in
653 this cellular compartment.

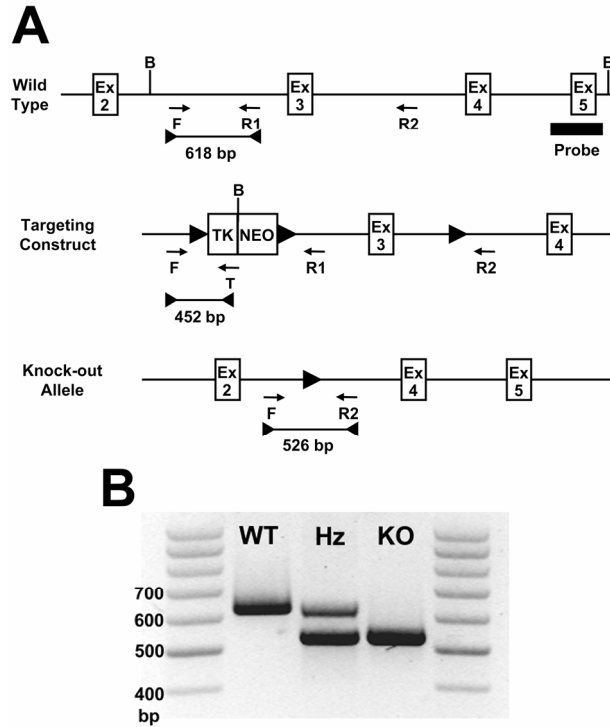


Figure 1

654

655

656

657

658

659

660

661

662

663

664

665

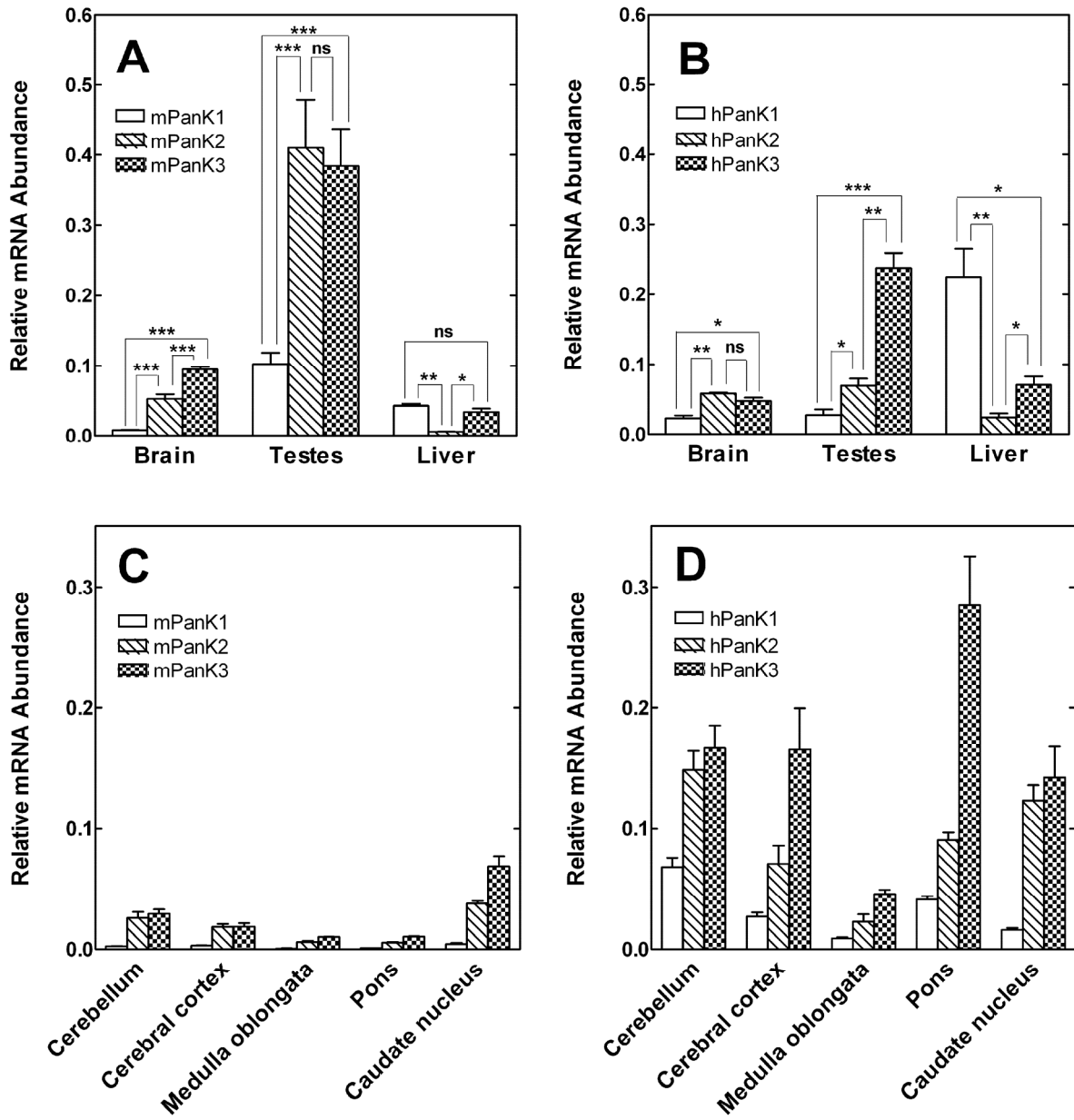


Figure 2

666
 667
 668
 669
 670
 671
 672

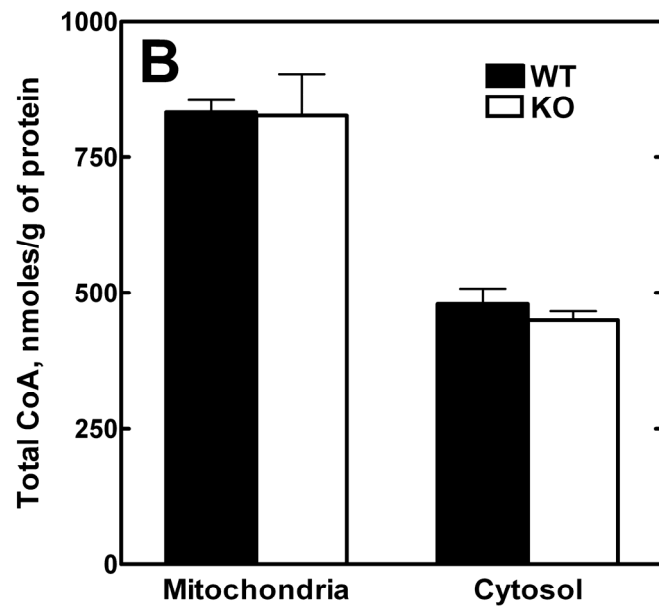
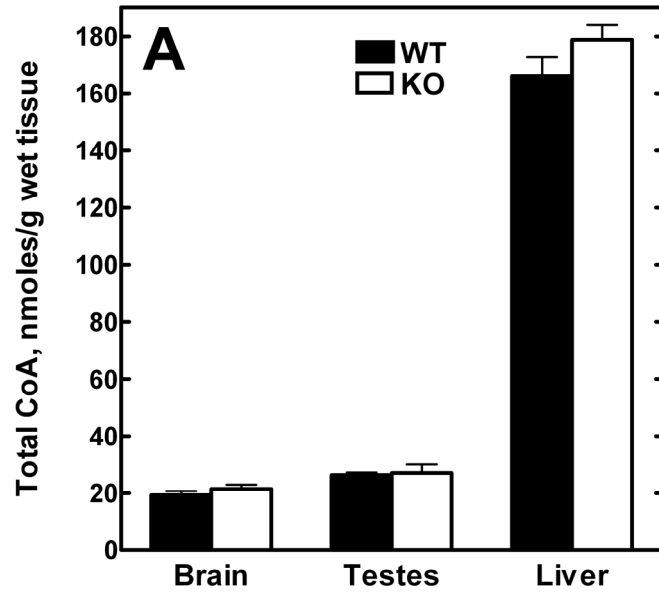


Figure 3

673

674

675

676

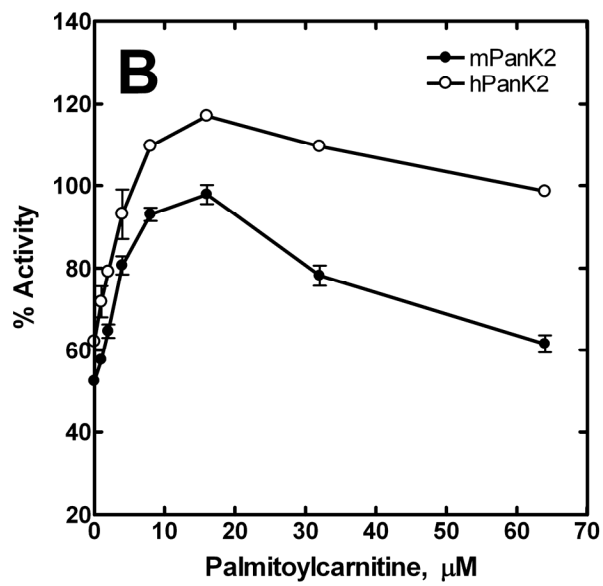
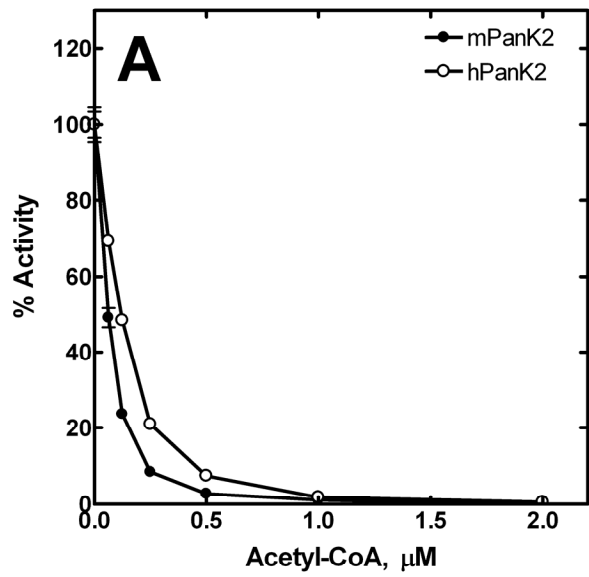


Figure 4

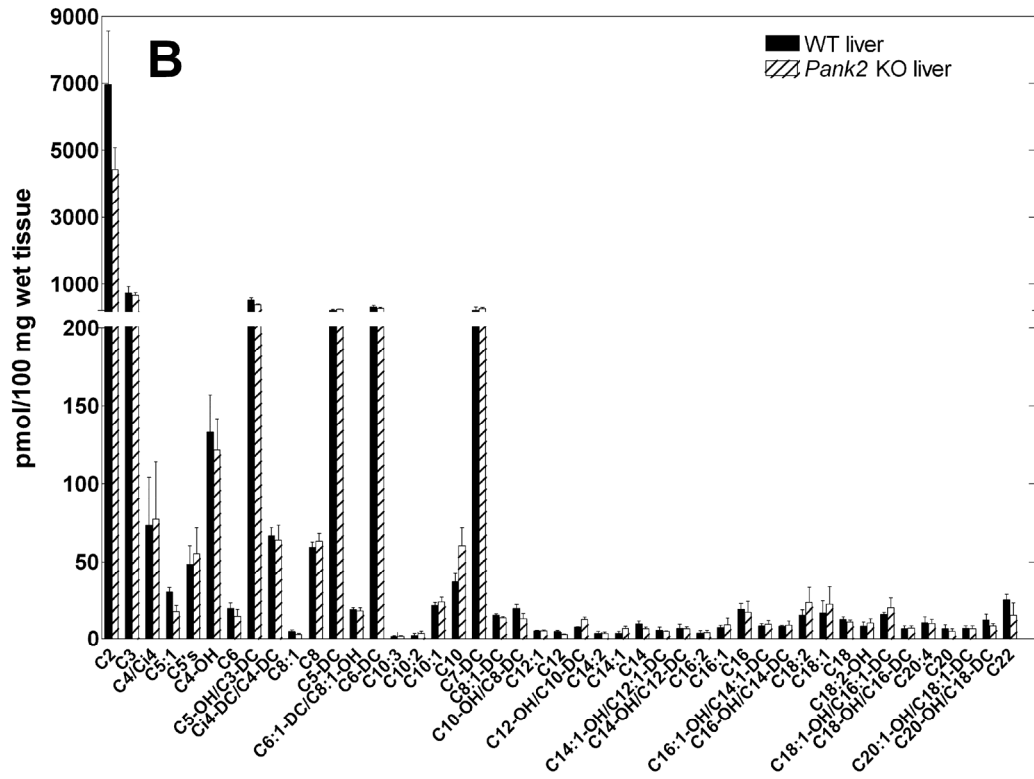
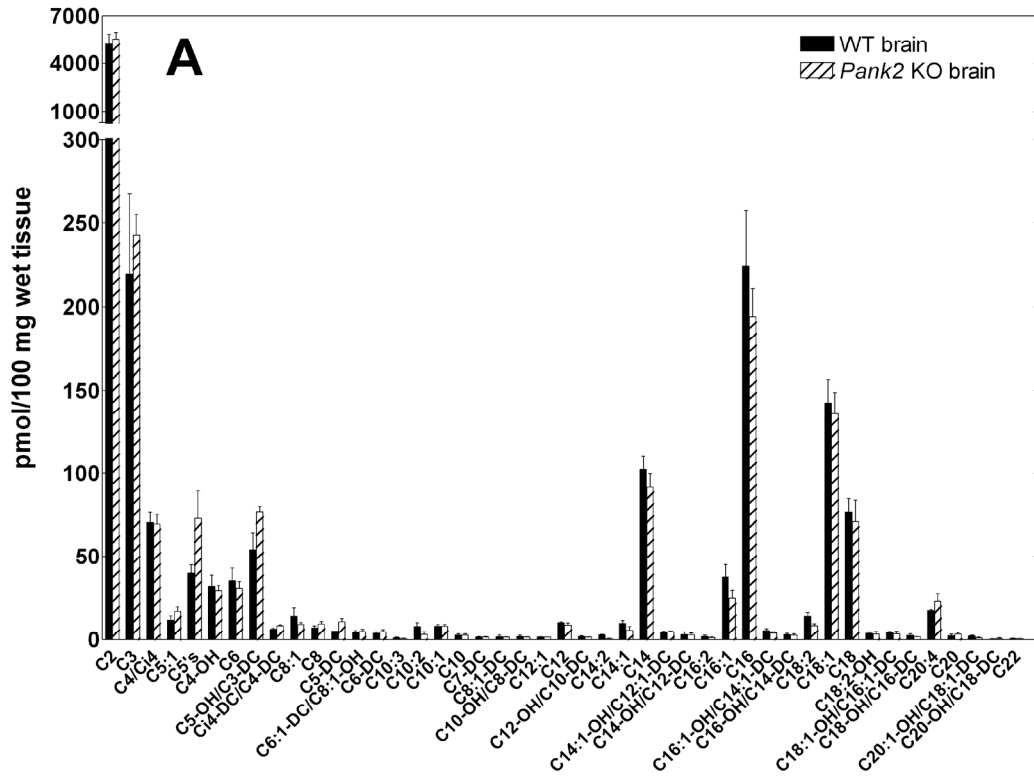
677

678

679

680

681



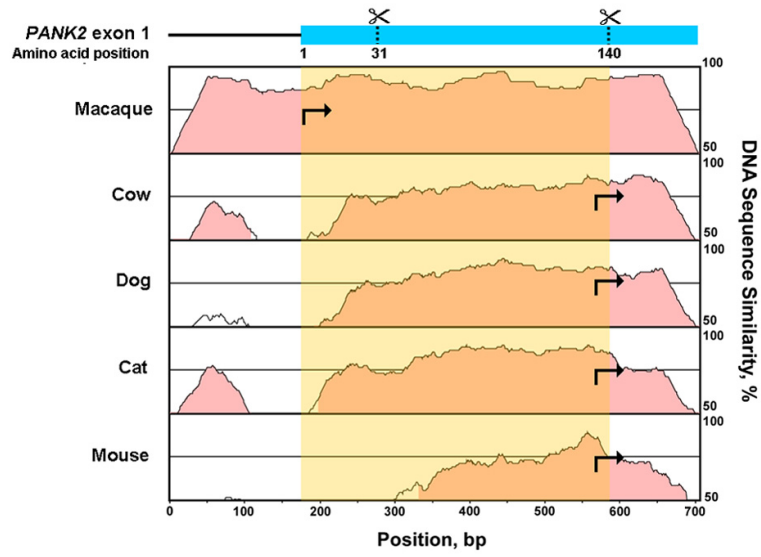
682

683

684

Figure 5

685



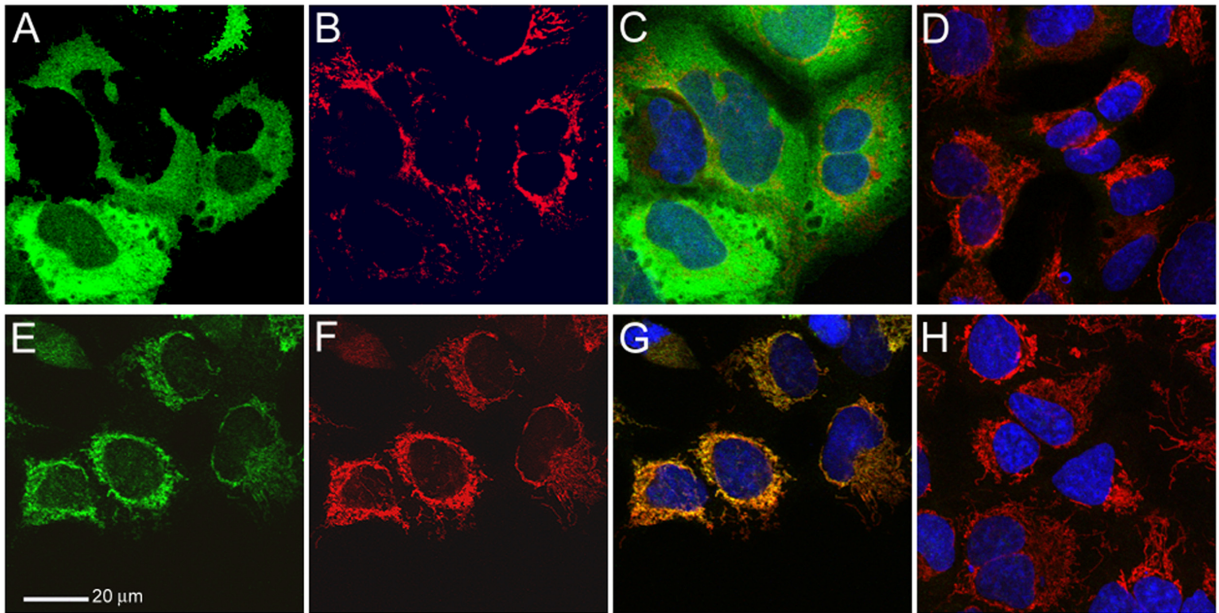
686

687

688

689

Figure 6



690

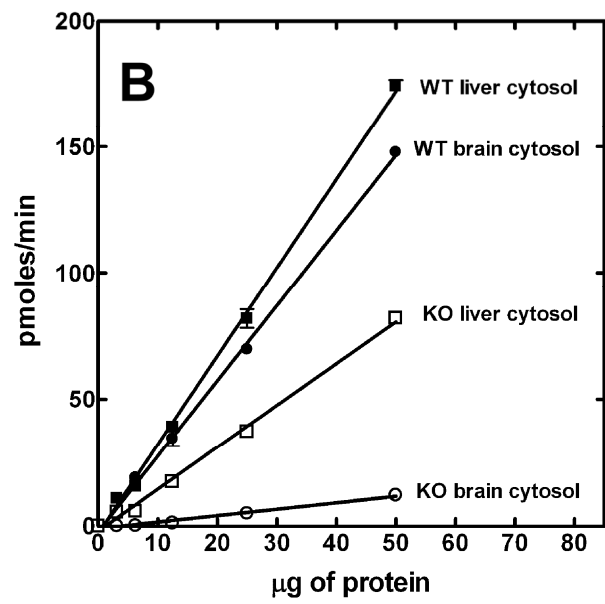
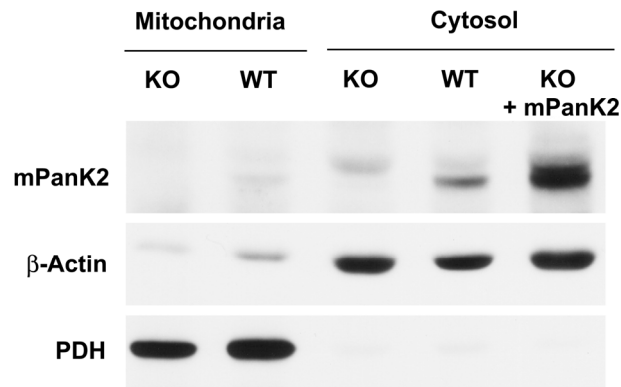
691

692

693

694

Figure 7

A**Figure 8**

695

696

697